Measurement of existing and new possible doubles based on Gaia DR3 during 2022 Q4

Gergely Talaber
Amateur astronomer, Bakonykuti, Hungary; gergely.talaber@gmail.com

Abstract

The paper focuses on the observation and measurement of existing and new possible double stars based on Gaia DR3 data. Double star identification in the latest Gaia data release (DR3) was done by data mining using Python programing language during 2022 October and based on several criteria and calculations. Measurements were done with an amateur telescope in Hungary during 2022 December.

1. Introduction

While imaging different WDS doubles, I noticed some double star-like objects on the images, which were not described in the Washington Double Star catalog. I found it strange, so I started to check these pairs using Skychart (Cartes du Ciel) and Aladin software, later directly in the Gaia DR3 archive. One of the accidentally found double star and its measures was published in 2023 January (Gergely Talaber et. al.). I decided to build a Python script to search for possible visual doubles in the Gaia database and measure them over the years. Data mining, even with the modern computers takes time considering the enormous amount of data, therefore I defined some criteria to focus only on relative bright stars not so far from the Sun, as the accuracy of the Gaia DR3 database is decreasing dramatically as the distance increases in case of point-like sources, where statistical analysis and related tools cannot be used. The magnitude was selected to be 15 or less, while the parallax was set to 0,5 mas or higher.

Accessing Gaia DR3 data and describe data mining process

The Gaia DR3 dataset is publicly available for use on the Gaia Archive webpage: https://cdn.gea.esac.esa.int/Gaia/gdr3/gaia_source/. One file contains approximately 500.000 sources. These files need to be downloaded and processed to get the double stars hiding between the lines. The required algorithm is quite simple.

1. Download and extract .tar.gz file
2. Filter out sources according to the selection criteria:
    a. Magnitude (phot_g_mean_mag) is 15 or less
    b. Parallax (parallax) is 0.5 mas or above
3. Search for pair of stars, where:
    a. The distance and distance calculation error based on the parallax and parallax error allows the sources to be on the same distance.
    b. The separation between the two star sources in respect of the calculated distance is less than 10.000 AU, despite the theoretical separation can exceed this distance. The limit had to be set somewhere to control the amount of data to be able to process it with a desktop computer within a suitable time period.

Selection of the measured pairs

The selection of the measured pairs was done in respect of the observable section of the night sky on the dates of observation. Furthermore, to make accurate measurements in respect of the telescope capabilities, the separation of the pairs in scope was selected to 5.0 arcsecond or higher and the visual magnitude to 13.0 or less.

Methods and calculations used to evaluate binarity

The base evaluation of binarity was done in the similar way, like the Plot Tool (version 3.20) with the extension of radial velocity calculation.

Parallax and Proper motion factors

Parallax factor is calculated according to Harshaw formula (R. Harshaw 2018.). Theoretically the similar are the parallaxes, the result is closer to 1.0.

$$P_{px} = 1 - \left| \frac{P_d - C_d}{\frac{1}{2}(P_d + C_d)} \right| \quad [1]$$

Where P_d is the distance of the Primary star from the Sun (parsecs), C_d is the distance of the Companion star from the Sun (parsecs).

Although the parallax is an important indicator of binarity, the proper motions of the components need to be taken into consideration. Stars with highly different proper motions will not be in each other's neighborhood for long, while common proper motions indicate that they are moving in the sky in the similar direction as we are expecting for stars, which are in gravitational bound. The Proper motion factor is calculated according to the Harshaw formula (R. Harshaw 2018.).

$$P_{pm} = \left| 1 - \frac{\sqrt{(P_{pmra} - C_{pmra})^2} + \sqrt{(P_{pmdec} - C_{pmdec})^2}}{\sqrt{P_{pmra}^2 + P_{pmdec}^2} + \sqrt{C_{pmra}^2 + C_{pmdec}^2}} \right| \quad [2]$$

Where P_{pmra} and P_{pmdec} are the proper motion vectors of the Primary star in RA and DEC directions, while C_{pmra} and C_{pmdec} are the proper motion vectors of the Companion star in RA and DEC directions.

Categories of the proper motion analysis are:

a) 0.8-1: Common Proper Motion (CPM)
b) 0.6-0.8: Similar Proper Motion (SPM)
c) 0.2-0.6: Different Proper Motion pairs (DPM)

Proper motion and radial velocity analysis

However, the proper motion factor tells us a lot about the nature of the pair, the following calculations can provide the exact determination of double star physicality. The method is based on the calculation of the differences of the tangential and radial velocities compared to the escape velocity of the system. Important to mention that radial velocity is not defined for several stars in Gaia DR3, in these cases we can evaluate the binarity based on the parallax and common proper motion factor, if historical data is not available. We need to take the accuracy of radial velocity and radial velocity error values into consideration, as in several cases, the error range is way too wide, therefore cannot be used for accurate

calculations. The accuracy of Gaia data will be increased in the upcoming data releases. For the time being, it is worth focusing on brighter stars with accurate data and develop methods and techniques, what can be used, when future data releases will be shared.

Tangential speed calculation is very simple based on Pythagoras theorem.

$$Pm_{tandif} = \sqrt{(P_{vra} - C_{vra})^2 + (P_{vdec} - C_{vdec})^2} \quad [3]$$

Where Pm_{tandif} is the difference in mas per year, P_{vra} and P_{vdec} are the proper motion vectors of the Primary star in RA and DEC directions, while C_{vra} and C_{vdec} are the proper motion vectors of the Companion star in RA and DEC directions. Important to mention, that as we are calculating in mas (milliarcseconds) per year, the speed difference is given also in mas per year, therefore adaptation to $km.s^{-1}$ is required.

$$V_{tandif} = 4.74372 * \frac{Pm_{tandif}}{P_{px}} \quad [4]$$

Where V_{tandif} will be the tangential speed difference in $km.s^{-1}$, Pm_{tandif} is the difference in mas per year and the P_{px} is the parallax of the system and 4.74372 is the constant to calculate the difference between AUs and $km.s^{-1}$. As mentioned earlier, Pm_{tandif} and P_{px} values are set in milliarcseconds as recorded in the Gaia DR3.

Out of these equations, the total difference of the tangential and radial vectors can be calculated with ease with the following equation.

$$\Sigma V_{diff} = \sqrt{V_{tandif}^2 + |P_{vrad} - C_{vrad}|^2} \quad [5]$$

Where $\sum V_{diff}$ is the total speed difference in $km.s^{-1}$, V_{tandif} will be the tangential speed difference in $km.s^{-1}$, P_{vrad} and C_{vrad} are the Primary and the Companion star's radial speed in $km.s^{-1}$.

To get the final verdict regarding the binarity of the pair, the system's escape velocity needs to be calculated.

$$V_{esc} = \sqrt{\frac{2GM_{tot}}{r}} \quad [6]$$

Where G is the gravitational constant, M_{tot} is the sum of the mass of the two stars in Sunmasses, finally r is the distance between the two stars in parsecs. Masses of the stars were defined based on the absolute magnitude and luminosity calculations of the Plot tool version 3.19 (Richard Harshaw 2020.).

Defining binarity seems straightforward from this point, if V_{esc} (escape velocity) is greater than V_{diff} (differential velocity), the system seems gravitationally bound based on the actual data. However, it needs to be noted, that the final evaluation depends on the continuous observations of these double stars till the historical data clearly shows the elliptical trajectories, and accurate orbits can be calculated.

2. Equipment and Methods

The telescope used for imaging was a Meade LX90 203/2000 mm Schmidt-Cassegrain on the factory azimuthal (fork) mount. The sensor used was a Canon 1000D, 10.1 Mpx dslr on ISO 1600 with 10.0 second exposures. No additional filter was applied. The number of images taken for each object was 10. The telescope and the camera were controlled by Kstars and Ekos using indilib drivers.

Processing of the images was done by the following sequence:

1. Identify the image scale, coordinates and orientation using astrometry.net software package. Images were processed in batch on a linux desktop machine with the help of bash scripting to automatize the procedure.
2. Identify sources and measurement of the pairs on the individual images was done by a custom script written in Python programing language using os, sys, astropy, photutils, astroquery, math and numpy libraries.

Observations were done on the clear nights of 7th (2022.341) 17th (2022.351) and 28th (2022.362) of December 2022.

Examples

Two images are attached to illustrate the imaging results as the base of measurements.

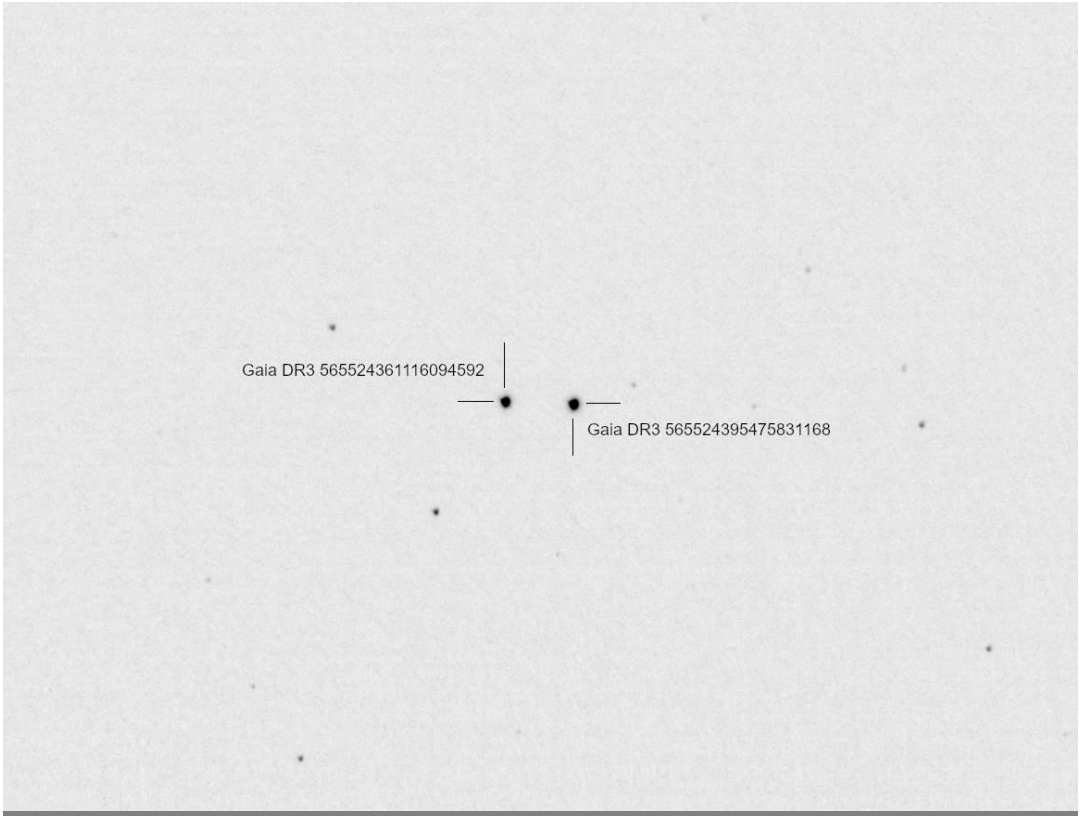

The image shows the 01099+7936 SKF 2036 AB components measured on the 7th of December 2022 (2022.341).

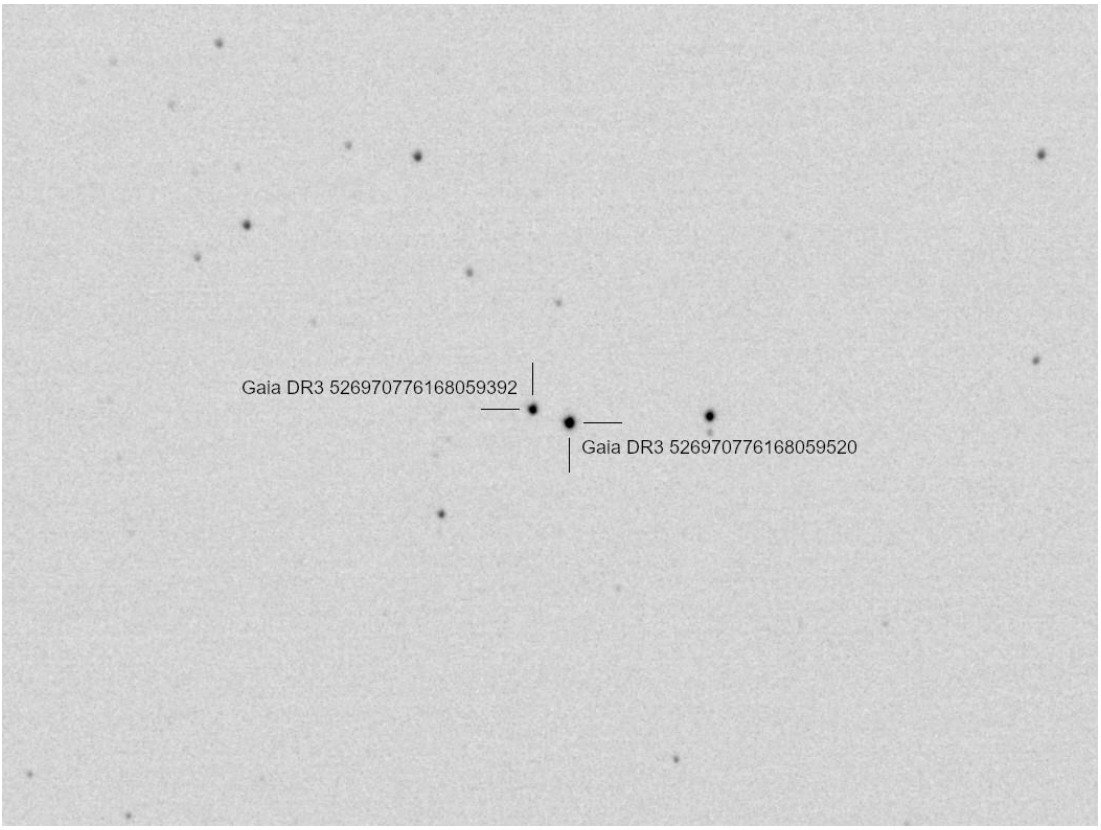

The image shows the candidate 2212A1 components measured on the 7th of December 2022 (2022.341).

3. Data

Explanation of the table fields

Table 1.

- WDS Identifier: WDS coordinates + Discoverer + Components.
- Position angle (Theta): mean measured position angle of the components in decimal degrees.
- Position angle std. error: standard error of the position angle measurements in decimal degrees.
- Separation: mean measured separation of the components in arcseconds.
- Separation std. error: standard error of the separation measurements in arcseconds.
- Physical separation: weighted separation in AU.

Table 2.

- WDS Identifier: WDS identifier + Discoverer + Components.
- Measured magnitude: relative magnitude of the star compared to the image background. The higher is the absolute value, the brighter the star.
- Std. error: standard error of the magnitude measurements.
- Apparent magnitude: the components G magnitude in the Gaia DR3 (g_phot_mean_mag)
- Absolute magnitude: calculated value based on the apparent magnitude and the distance of the star.

- Luminosity: calculated value based on the apparent magnitude and the distance of the star.
- Mass: calculated value based on the apparent magnitude and the distance of the star.
- Date of observation: date of the observation night in <year>.<day of the year> format.

WDS pairs

Table 1. - WDS pairs

WDS Identifier	Position angle (Theta)	Position angle std. error	Separation (Rho)	Separation std. error	Physical separation
01099+7936 SKF2036 AB	96.254	0.0208	45.411	0.0188	8731.157
02579+6400 STI 409 AB	208.136	0.244	8.766	0.246	5381.416
02020+6028 SKF2784	246.840	0.126	33.860	0.083	5739.833
04596+8008 ARG 59	211.232	0.941	7.019	0.209	2341.968
04265+7847 BVD 144	343.958	0.241	13.054	0.034	2355.259
02096+6343 HJ 1106	74.093	0.499	9.560	0.108	1434.570
02145+6415 HJ 1111	342.615	0.619	7.209	0.036	5568.166
02336+6642 HJ 1118	128.358	0.672	6.808	0.191	2765.912
02443+6411 HJ 1122	216.498	0.428	10.224	0.061	422.539
02460+6749 HJ 1125	224.285	0.119	26.290	0.073	7750.267
02216+7212 HJ 2122	139.651	0.100	31.386	0.107	6379.392
03597+8215 HJL 54	41.832	0.079	24.045	0.038	4501.645
02053+6740 STF 199 AB	22.183	0.100	35.777	0.109	6506.360
02246+5959 STF 255	2.027	1.150	5.865	0.299	1269.551
02190+2047 UC 715	268.810	0.752	6.497	0.418	547.746
02260+2324 UC 738 AC	215.764	0.067	54.730	0.081	4260.222
02363+2905 GRV 135	262.678	0.120	19.948	0.086	7185.815
04572+2030 HJ 2245	190.704	0.118	27.016	0.049	3569.497
05000+2426 KPP1111	210.641	0.925	8.745	0.350	2210.824
04598+2434 POU 508	110.308	1.522	6.723	0.214	4289.996
04557+2211 LAR 1	212.723	0.148	15.063	0.044	7556.586
02448+2852 LDS 880	207.391	0.287	35.502	0.107	5083.884
03416+2655 LDS6095	35.667	0.115	40.514	0.093	5891.657
02019+2430 POU 156	203.694	0.770	13.520	0.188	2168.138
02204+2456 POU 175	46.706	0.765	11.999	0.124	2574.947
02398+2522 POU 214	234.445	2.061	7.739	0.352	4556.139
02595+2440 POU 232	210.368	1.062	14.194	0.752	2668.206
04574+2423 POU 504	73.546	0.226	17.933	0.081	6207.523
04563+2415 LDS 6148	181.901	0.132	41.309	0.187	6707.637
02097+2021 STF 221 AB	145.128	0.679	8.228	0.089	2128.816
02089+2031 CHE 61	203.756	1.085	10.013	0.196	3378.148
02190+2047 UC 715	268.810	0.752	6.497	0.418	547.746
02260+2324 POU 187 AB	215.764	0.067	54.730	0.081	4260.222

Table 2. - WDS pairs

WDS Identifier	Component source id	Measured magnitude	Std. error	Apparent magnitude	Absolute magnitude	Luminosity	Mass	Date of observation
01099+7936	565524395475831168	-4.664	0.0222	8.984	2.557	8.171	1.69	2022.341
SKF2036 AB	565524361116094592	-4.373	0.0414	9.324	2.902	5.936	1.56	2022.341
02579+6400	467885220313421952	-4.304	0.595	9.450	0.548	52.318	2.814	2022.351
STI 409 AB	467885220313423488	-3.101	0.607	10.604	1.675	18.466	2.090	2022.351
02020+6028	507980492369928320	-4.326	0.415	8.980	2.827	6.368	1.589	2022.351
SKF2784	507980492374331776	-2.963	0.418	10.257	4.109	1.948	1.181	2022.351
04596+8008	556461636524260224	-2.320	0.182	10.103	2.667	7.383	1.648	2022.351
ARG 59	556461636524260352	-1.961	0.219	10.364	2.936	5.759	1.549	2022.351
04265+7847	556269634303988608	-3.215	0.087	10.886	4.609	1.226	1.052	2022.351
BVD 144	556269703025227264	-2.402	0.075	11.701	5.417	0.581	0.873	2022.351
02096+6343	514965517944096768	-2.344	0.328	11.599	5.721	0.439	0.814	2022.351
HJ 1106	514965513638516608	-1.959	0.340	11.885	6.001	0.339	0.763	2022.351
02145+6415	515193460450555008	-3.576	0.125	10.593	1.173	29.366	2.386	2022.351
HJ 1111	515194937917766016	-2.649	0.165	11.452	1.993	13.769	1.926	2022.351
02336+6642	516996831311800192	-2.278	0.195	11.653	3.664	2.937	1.309	2022.351
HJ 1118	516996831311800576	-1.754	0.241	12.124	4.147	1.880	1.171	2022.351
02443+6411	515708925243186560	-4.468	0.327	9.220	6.138	0.299	0.739	2022.351
HJ 1122	515708925243187072	-2.939	0.333	10.503	7.421	0.091	0.549	2022.351
02460+6749	517531022162318592	-5.214	0.308	8.477	1.113	31.044	2.424	2022.351
HJ 1125	517530987802580736	-2.519	0.467	11.439	4.080	2.001	1.189	2022.351
02216+7212	546234219880801024	-3.860	0.337	10.096	3.559	3.239	1.341	2022.351
HJ 2122	546234219881683584	-3.876	0.331	10.108	3.564	3.222	1.340	2022.351
03597+8215	569810390583019008	-4.438	0.243	9.607	3.248	4.316	1.441	2022.351
HJL 54	569810493662233984	-3.887	0.225	10.152	3.761	2.686	1.280	2022.351
02053+6740	520472353205614848	-3.977	0.547	9.070	2.773	6.692	1.608	2022.351
STF 199 AB	520472456284824320	-3.748	0.536	9.277	2.971	5.574	1.537	2022.351
02246+5959	459340365699412992	-2.356	0.237	10.357	3.989	2.176	1.214	2022.351
STF 255	459340365699412096	-1.885	0.252	10.711	4.346	1.563	1.118	2022.351
02190+2047	99276730233633408	-2.129	0.181	11.489	6.985	0.136	0.608	2022.362
UC 715	99276725938999296	-0.620	0.202	12.599	8.098	0.049	0.470	2022.362
02260+2324	101754651485587968	-2.938	0.205	10.693	6.234	0.273	0.723	2022.362
UC 738 AC	101660810744934528	-2.256	0.235	11.216	6.768	0.167	0.639	2022.362
02363+2905	128284698832967552	-3.008	0.181	10.500	2.699	7.170	1.636	2022.362
GRV 135	128284698832968064	-2.411	0.185	11.124	3.345	3.945	1.409	2022.362
04572+2030	3408652278519858304	-4.450	0.203	9.404	3.796	2.600	1.270	2022.362
HJ 2245	3408652278519858560	-2.273	0.185	11.503	5.888	0.376	0.783	2022.362
05000+2426	3419571945108713472	-1.162	0.107	12.483	5.469	0.554	0.863	2022.362
KPP1111	3419571562855171328	-0.201	0.158	13.440	6.438	0.226	0.690	2022.362
04598+2434	3419582596627546496	-1.165	0.203	12.464	3.551	3.263	1.344	2022.362
POU 508	3419582596627545472	-0.971	0.176	12.703	3.765	2.677	1.279	2022.362
04557+2211	3412430544070253056	-4.925	0.213	9.131	0.625	48.727	2.757	2022.362
LAR 1	3412430170409736064	-3.348	0.247	10.703	2.181	11.571	1.844	2022.362
02448+2852	128738140004444416	-1.271	0.150	12.056	6.283	0.261	0.715	2022.362
LDS 880	128738105644706304	-1.166	0.216	12.090	6.308	0.255	0.711	2022.362
03416+2655	71091879232277888	-2.623	0.306	10.908	5.084	0.791	0.943	2022.362
LDS6095	71091913592016128	-2.033	0.262	11.753	5.926	0.363	0.776	2022.362
02019+2430	104891042763689088	-2.164	0.281	11.430	5.377	0.603	0.881	2022.362
POU 156	104891004108145024	-1.941	0.282	11.646	5.608	0.487	0.836	2022.362
02204+2456	102899135715338880	-3.046	0.205	10.434	3.773	2.657	1.277	2022.362
POU 175	102899517968038144	-1.108	0.225	12.241	5.584	0.498	0.840	2022.362

02398+2522	126152329174120192	-1.410	0.175	12.369	3.545	3.278	1.346	2022.362
POU 214	126152230390423680	-0.836	0.169	12.935	4.104	1.955	1.183	2022.362
02595+2440	113341816119945216	-1.658	0.361	11.771	5.327	0.632	0.891	2022.362
POU 232	113341820415458432	-1.001	0.288	12.392	5.950	0.355	0.772	2022.362
04574+2423	3419489413016911616	-4.576	0.319	9.152	1.438	22.989	2.225	2022.362
POU 504	3419488657102664320	-2.154	0.320	11.499	3.799	2.594	1.269	2022.362
04563+2415	3419649357600434048	-2.276	0.193	10.596	4.532	1.317	1.071	2022.362
LDS 6148	3419649288879598592	-1.319	0.177	11.491	5.425	0.577	0.872	2022.362
02097+2021	93427706330915456	-5.006	0.056	7.955	0.949	36.144	2.532	2022.362
STF 221 AB	93427706330915584	-4.335	0.244	9.420	2.397	9.479	1.755	2022.362
02089+2031	93439766598535168	-2.196	0.316	11.479	3.833	2.513	1.259	2022.362
CHE 61	93439766599233280	-1.318	0.305	12.312	4.666	1.164	1.039	2022.362
02190+2047	99276730233633408	-2.129	0.181	11.489	6.985	0.136	0.608	2022.362
UC 715	99276725938999296	-0.620	0.202	12.599	8.098	0.049	0.470	2022.362
02260+2324	101754651485587968	-2.938	0.205	10.693	6.234	0.273	0.723	2022.362
POU 187 AB	101660810744934528	-2.256	0.235	11.216	6.768	0.167	0.639	2022.362

New candidates

In the tables of the new pairs, the WDS identifier column is replaced of the new pair's temporary name, which describes the last two digits of the year of the observation + the month of the observation, the alphabet code represents the sequence of the observation session (A is for the first observation in the month, B is for the second, etc.) and finally the last number represents the image set of the particular observation session.

Table 1. – New candidates

Name	Position angle (Theta)	Position angle std. error	Separation (Rho)	Separation std. error	Physical separation
2212A1	77.114	0.195	22.981	0.064	7395.777
2212B1	204.885	0.960	22.742	0.468	9649.497
2212B4	287.506	0.171	25.313	0.095	7905.710
2212B5	81.299	1.782	7.710	0.386	3775.942
2212B6	116.738	0.806	9.258	0.427	3114.027
2212B7	148.920	0.371	19.291	0.162	9437.215
2212B8	111.637	0.634	13.402	0.202	4956.259
2212B9	295.091	0.780	6.355	0.306	374.644
2212B10	244.061	0.233	43.224	0.089	9623.245
2212B11	278.408	1.296	6.767	0.402	2818.622
2212B12	80.424	0.612	13.880	0.159	5498.501
2212B13	47.075	0.105	22.827	0.053	7523.986
2212B14A	149.026	0.191	36.005	0.202	9916.335
2212B14B	131.591	0.130	43.031	0.107	2617.279
2212B15	278.326	0.870	6.258	0.125	8160.251
2212B16	175.819	0.486	10.563	0.119	5042.579
2212B17	281.591	0.332	13.277	0.051	6251.981
2212B18	137.443	0.258	23.174	0.061	5432.274
2212B19	111.582	1.094	4.609	0.149	3584.018
2212B20	157.052	0.243	24.914	0.121	3219.655
2212B21	273.639	1.022	12.132	0.265	3971.752
2212B22	226.101	0.357	14.797	0.079	7861.432
2212B23	329.449	0.328	6.152	0.110	4061.953
2212B24	148.108	0.101	138.652	0.196	9029.131

2212C1	13.944	1.102	9.375	0.227	2568.243
2212C2	12.663	0.438	9.071	0.153	6757.681
2212C3	94.104	0.413	16.633	0.129	6203.598
2212C4	154.231	0.352	22.874	0.114	4705.496
2212C5	7.542	0.244	19.417	0.108	7741.998
2212C8	63.005	1.198	9.089	0.213	5422.652
2212C9	43.555	0.466	13.518	0.142	8022.146
2212C10	60.445	0.562	6.758	0.360	1661.785
2212C11	345.827	2.261	5.152	0.253	840.640
2212C12	40.580	0.760	16.132	0.263	7735.262
2212C13	194.829	1.444	5.636	0.470	3304.171
2212C14	101.071	0.233	41.704	0.084	4284.366
2212C15	47.183	1.516	32.474	0.487	3986.848
2212C16	21.379	2.158	5.101	0.312	2927.490
2212C17	120.650	0.446	23.251	0.170	4688.106
2212C18	147.289	1.520	5.660	0.199	2463.439
2212C19	265.075	0.184	41.767	0.153	9234.187
2212C20	171.106	0.670	9.337	0.145	3456.324

Table 2. – New candidates

Name	Component source id	Measured magnitude	Std. error	Apparent magnitude	Absolute magnitude	Luminosity	Mass	Date of observation
2212A1	526970776168059520	-3.508	0.053	10.108	2.562	8.137	1.689	2022.341
	526970776168059392	-2.457	0.052	11.031	3.483	3.474	1.365	2022.341
2212B1	465169460951515904	-0.742	0.308	12.266	4.142	1.888	1.172	2022.351
	465169426591780480	-0.406	0.241	12.576	4.466	1.400	1.088	2022.351
2212B4	508559930693790720	-2.068	0.426	11.574	4.083	1.995	1.188	2022.351
	508559934999464960	-1.978	0.433	11.609	4.116	1.935	1.179	2022.351
2212B5	513644282914705792	-1.313	0.345	12.164	3.836	2.506	1.258	2022.351
	513644278622548992	-0.836	0.407	12.668	4.333	1.583	1.122	2022.351
2212B6	513664417727270912	-1.430	0.501	12.043	4.438	1.437	1.095	2022.351
	513664417727796224	-0.717	0.428	12.882	4.999	0.855	0.962	2022.351
2212B7	515660404987468032	-1.953	0.411	11.384	2.931	5.786	1.551	2022.351
	515660404987468160	-1.174	0.441	12.189	3.721	2.786	1.292	2022.351
2212B8	515924566960262016	-3.843	0.192	10.265	2.403	9.419	1.752	2022.351
	515924566959376768	-0.893	0.253	12.894	5.058	0.810	0.949	2022.351
2212B9	516128010972653824	-4.769	0.222	9.124	5.379	0.602	0.881	2022.351
	516128010970194944	-4.651	0.230	9.191	5.447	0.565	0.867	2022.351
2212B10	516690303785992832	-1.591	0.240	12.417	5.679	0.456	0.822	2022.351
	516690514243067904	-1.087	0.239	12.900	6.157	0.293	0.736	2022.351
2212B11	517580637625449216	-2.974	0.346	10.913	2.983	5.512	1.532	2022.351
	517580633328641280	-1.356	0.394	12.344	4.416	1.467	1.101	2022.351
2212B12	517862009521987840	-3.943	0.504	9.417	1.467	22.393	2.208	2022.351
	517862009521986688	-1.324	0.558	11.868	3.864	2.442	1.250	2022.351
2212B13	542506493208226048	-3.587	0.109	10.682	3.085	5.018	1.497	2022.351
	542506493208225920	-3.363	0.103	10.846	3.246	4.322	1.442	2022.351
2212B14A	545755451286740096	-2.108	0.175	11.958	4.752	1.075	1.018	2022.351
	545755446988985984	-0.629	0.227	13.201	5.994	0.341	0.764	2022.351
2212B14B	547259480114344832	-5.053	0.103	7.942	4.017	2.119	1.207	2022.351
	547259407097385216	-4.203	0.183	9.888	5.965	0.350	0.769	2022.351
2212B15	549209704503767808	-2.425	0.140	11.474	0.919	37.159	2.552	2022.351
	549209700208689152	-1.118	0.161	12.807	2.275	10.606	1.805	2022.351
2212B16	549323499660422400	-1.538	0.198	12.567	4.157	1.863	1.168	2022.351
	549323499660422784	-1.536	0.125	12.598	4.195	1.798	1.158	2022.351

2212B17	550312755184884736	-4.639	0.046	9.270	0.890	38.154	2.571	2022.351
	550312819607732480	-2.027	0.050	12.041	3.673	2.914	1.307	2022.351
2212B18	550516680231922304	-2.686	0.167	11.467	4.611	1.225	1.052	2022.351
	550513720997555840	-1.722	0.176	12.327	5.470	0.553	0.862	2022.351
2212B19	552103099415828224	-1.725	0.095	12.305	3.048	5.189	1.509	2022.351
	552103103711528448	-1.219	0.088	12.817	3.558	3.241	1.342	2022.351
2212B20	557820186218618368	-4.308	0.103	9.940	4.381	1.514	1.109	2022.351
	557820181921933952	-1.024	0.139	12.857	7.298	0.102	0.565	2022.351
2212B21	568218989237713408	-1.257	0.134	11.200	3.627	3.040	1.320	2022.351
	568218989237713920	-0.618	0.166	11.768	4.196	1.797	1.158	2022.351
2212B22	571140907028561152	-3.055	0.291	10.825	2.182	11.560	1.844	2022.351
	571140907028561920	-2.146	0.326	11.801	3.167	4.650	1.468	2022.351
2212B23	572964545846243072	-2.151	0.141	11.793	2.739	6.909	1.621	2022.351
	572964545850231040	-2.120	0.170	11.804	2.737	6.920	1.622	2022.351
2212B24	541801332594262912	-5.057	0.100	6.229	2.155	11.853	1.855	2022.351
	541801057716360832	-0.768	0.282	12.700	8.634	0.030	0.411	2022.351
2212C1	70583050164231296	-1.031	0.235	12.404	5.235	0.688	0.911	2022.362
	70588921381165952	-0.553	0.211	12.789	5.616	0.484	0.834	2022.362
2212C2	70592258574077440	-1.824	0.198	11.819	2.481	8.771	1.721	2022.362
	70592254276654976	-1.655	0.207	11.950	2.587	7.953	1.679	2022.362
2212C3	85103509955568000	-2.460	0.192	11.463	3.607	3.097	1.327	2022.362
	85103544315306240	-1.259	0.175	12.616	4.751	1.075	1.018	2022.362
2212C4	86663338998258816	-3.025	0.121	10.880	4.256	1.699	1.142	2022.362
	86663270278782464	-0.809	0.163	12.829	6.252	0.269	0.720	2022.362
2212C5	88427333605920384	-2.307	0.188	11.311	3.367	3.866	1.402	2022.362
	88427333606422912	-2.234	0.136	11.412	3.390	3.786	1.395	2022.362
2212C8	103750844909960192	-1.045	0.263	12.490	3.644	2.991	1.315	2022.362
	103750947989175040	-1.012	0.194	12.638	3.776	2.649	1.276	2022.362
2212C9	114831035899953920	-1.647	0.174	12.085	3.276	4.204	1.432	2022.362
	114831413857075840	-1.302	0.216	12.454	3.597	3.125	1.330	2022.362
2212C10	127498204421532800	-3.174	0.256	10.146	3.378	3.827	1.399	2022.362
	127498238781271040	-2.483	0.286	10.759	3.983	2.188	1.216	2022.362
2212C11	128620870218113536	-1.354	0.180	12.119	6.308	0.255	0.711	2022.362
	128620870221374464	-1.088	0.225	12.301	6.488	0.216	0.682	2022.362
2212C12	130975027692042368	-1.463	0.330	12.059	3.637	3.013	1.317	2022.362
	130975031987363072	-1.241	0.319	12.315	3.892	2.379	1.242	2022.362
2212C13	166682256217174656	-4.349	0.237	9.282	0.673	46.614	2.722	2022.362
	166682256217677824	-4.360	0.244	9.282	0.646	47.814	2.742	2022.362
2212C14	166865496701799168	-2.399	0.205	11.429	6.376	0.240	0.700	2022.362
	166865393622583680	-1.331	0.211	12.301	7.242	0.108	0.573	2022.362
2212C15	167549908330274176	-2.716	0.407	10.879	5.416	0.582	0.873	2022.362
	167549942690010368	-1.505	0.413	12.036	6.570	0.200	0.669	2022.362
2212C16	167775376934171520	-1.332	0.091	12.428	3.972	2.211	1.219	2022.362
	167775372636909952	-0.602	0.158	12.963	4.474	1.389	1.086	2022.362
2212C17	300226769565257856	-0.883	0.190	12.350	5.800	0.408	0.799	2022.362
	300226773861342976	-0.891	0.162	12.436	5.916	0.366	0.778	2022.362
2212C18	3410268560613954304	-1.845	0.269	11.707	3.697	2.849	1.299	2022.362
	3410268457534739072	-1.425	0.236	12.104	4.097	1.969	1.185	2022.362
2212C19	3411148861405957248	-2.977	0.371	10.674	3.941	2.275	1.228	2022.362
	3411336152043815552	-1.160	0.360	12.317	5.598	0.492	0.837	2022.362
2212C20	3412544622698643328	-4.067	0.372	9.317	1.461	22.517	2.211	2022.362
	3412544622698644224	-2.869	0.393	10.645	2.789	6.596	1.603	2022.362

4. Discussion

Table 3.

- WDS Identifier: WDS identifier + Discoverer + Components.
- Parallax factor: calculated parallax factor based on equation [1].
- Proper motion factor: calculated proper motion factor based on equation [2].
- Proper motion category: calculated proper motion category.
- Escape velocity: system escape velocity based on star mass calculation.
- Relative velocity: system relative velocity calculated based on the relative differences of the proper motion and radial velocity vectors.
- Harshaw factor: calculated based on the weighted parallax factor (0.75) and proper motion factor (0.15). The maximum value of the factor for new pairs is 0.9, as historical data is not available, which is weighted for 0.1.
- Harshaw physicality: category of the pair's nature based on the calculated Harshaw factor.
- Binarity: calculated result based on the comparison of the escape and relative velocities.
    - yes: 3d vector calculations indicate that the pair is physical.
    - no: 3d vector calculations indicates that the pair is optical.
    - n/a: physicality of the pair based on 3d vector calculations cannot be determined due to the lack of accurate data. Important to mention, that many of the stars in the Gaia DR3 has no radial velocity value, or the error is way above the acceptable accuracy level, therefore "Binarity = n/a" means that we cannot be sure about the pair's gravitational bound at this point of time.

In the tables of the new pairs, the WDS identifier column is replaced of the new pair's temporary name, which describes the last two digits of the year of the observation + the month of the observation, the alphabet code represents the sequence of the observation session (A is for the first observation in the month, B is for the second, etc.) and finally the last number represents the image set of the particular observation session.

Table 3. – WDS pairs

WDS Identifier	Parallax factor	Proper motion factor	Proper motion category	Escape velocity	Relative velocity	Harshaw factor	Harshaw physicality	Binarity
01099+7936 SKF 2036 AB	0.997	0.999	CPM	0.8128	1.731	89.783	yes	n/a
02579+6400 STI 409 AB	0.987	0.997	CPM	1.271	n/a	89.030	yes	n/a
02020+6028 SKF 2784	0.998	0.998	CPM	0.925	1.489	89.820	yes	n/a
04596+8008 ARG 59	0.996	0.997	CPM	1.556	0.809	89.704	yes	yes
04265+7847 BVD 144	0.996	0.999	CPM	1.204	0.830	89.735	yes	yes
02096+6343 HJ 1106	0.997	0.999	CPM	1.396	4.470	89.778	yes	no
02145+6415 HJ 1111	0.982	0.978	CPM	1.172	3.978	88.339	yes	n/a
02336+6642 HJ 1118	0.994	0.997	CPM	1.261	5.323	89.562	yes	no
02443+6411 HJ 1122	0.999	0.999	CPM	2.326	0.563	89.956	yes	yes
02460+6749 HJ 1125	0.998	0.997	CPM	0.909	1.876	89.812	yes	n/a
02216+7212 HJ 2122	0.996	0.999	CPM	0.864	0.476	89.759	yes	yes
03597+8215 HJL 54	0.985	0.999	CPM	1.036	0.906	88.897	yes	yes
02053+6740 STF 199 AB	0.995	0.985	CPM	0.926	8.500	89.477	yes	no
02246+5959 STF 255	0.998	0.992	CPM	1.806	n/a	89.769	yes	n/a
02190+2047 UC 715	0.999	0.999	CPM	1.868	0.873	89.884	yes	yes
02260+2324 UC 738 AC	0.995	0.998	CPM	0.753	5.179	89.586	yes	n/a
02363+2905 GRV 135	0.990	0.997	CPM	0.867	1.963	89.169	yes	n/a
04572+2030 HJ 2245	0.996	1.000	CPM	1.010	n/a	89.732	yes	n/a
05000+2426 KPP 1111	0.995	0.999	CPM	1.116	15.224	89.573	yes	no
04598+2434 POU 508	0.988	0.994	CPM	1.042	6.136	89.022	yes	no
04557+2211 LAR 1	0.992	0.959	CPM	1.039	9.849	88.809	yes	no

02448+2852 LDS 880	0.996	1.000	CPM	0.705	0.520	89.694	yes	yes
03416+2655 LDS6095	0.999	1.000	CPM	0.720	n/a	89.927	yes	n/a
02019+2430 POU 156	0.993	0.965	CPM	1.185	42.389	88.952	yes	no
02204+2456 POU 175	0.998	1.000	CPM	1.208	0.479	89.864	yes	yes
02398+2522 POU 214	0.997	0.997	CPM	0.992	1.399	89.727	yes	n/a
02595+2440 POU 232	0.999	0.999	CPM	1.052	3.387	89.936	yes	n/a
04574+2423 POU 504	0.994	1.000	CPM	0.999	n/a	89.521	yes	n/a
04563+2415 LDS 6148	0.999	1.000	CPM	0.717	0.435	89.943	yes	yes
02097+2021 STF 221 AB	0.993	0.994	CPM	1.890	n/a	89.362	yes	n/a
02089+2031 CHE 61	1.000	1.000	CPM	1.099	0.401	89.966	yes	yes
02190+2047 UC 715	0.999	0.999	CPM	1.868	0.873	89.884	yes	yes
02260+2324 POU 187 AB	0.995	0.998	CPM	0.753	5.179	89.586	yes	no

Table 3. – New candidates

Name	Parallax factor	Proper motion factor	Proper motion category	Escape velocity	Relative velocity	Harshaw factor	Harshaw physicality	Binarity
2212A1	0.999	0.999	CPM	0.855	1.709	89.908	yes	no
2212B1	0.994	0.997	CPM	0.645	1.564	89.472	yes	n/a
2212B4	0.999	0.998	CPM	0.729	1.998	89.901	yes	n/a
2212B5	0.997	0.984	CPM	1.057	0.424	89.512	yes	yes
2212B6	0.872	0.823	CPM	1.082	60.421	77.763	yes	no
2212B7	0.993	0.996	CPM	0.731	4.518	89.445	yes	no
2212B8	0.988	0.993	CPM	0.983	1.873	89.021	yes	n/a
2212B9	1.000	1.000	CPM	2.877	1.612	89.965	yes	yes
2212B10	0.998	0.997	CPM	0.536	n/a	89.788	yes	n/a
2212B11	0.999	0.978	CPM	1.287	13.111	89.611	yes	n/a
2212B12	0.976	0.976	CPM	1.056	4.812	87.804	yes	no
2212B13	0.999	1.000	CPM	0.832	2.012	89.920	yes	no
2212B14A	0.999	0.999	CPM	0.565	0.232	89.941	yes	yes
2212B14B	1.000	0.998	CPM	1.157	n/a	89.947	yes	n/a
2212B15	0.989	0.994	CPM	0.973	10.376	89.089	yes	no
2212B16	0.996	0.999	CPM	0.905	0.669	89.718	yes	yes
2212B17	0.994	0.988	CPM	1.049	3.377	89.405	yes	no
2212B18	1.000	0.986	CPM	0.791	4.478	89.761	yes	no
2212B19	0.998	1.000	CPM	1.188	0.069	89.879	yes	yes
2212B20	1.000	1.000	CPM	0.961	n/a	89.983	yes	n/a
2212B21	1.000	0.999	CPM	1.052	0.647	89.984	yes	yes
2212B22	0.996	0.985	CPM	0.865	2.103	89.462	yes	n/a
2212B23	0.994	1.000	CPM	1.190	0.536	89.563	yes	yes
2212B24	0.996	0.999	CPM	0.667	n/a	89.691	yes	n/a
2212C1	0.998	1.000	CPM	1.098	0.789	89.841	yes	yes
2212C2	0.988	0.833	CPM	0.945	1.510	86.625	yes	n/a
2212C3	0.996	0.999	CPM	0.819	1.394	89.690	yes	n/a
2212C4	0.979	0.998	CPM	0.838	4.732	88.367	yes	n/a
2212C5	0.964	0.998	CPM	0.801	5.265	87.259	yes	n/a
2212C8	0.993	0.995	CPM	0.921	3.651	89.363	yes	n/a
2212C9	0.978	0.978	CPM	0.782	2.283	88.007	yes	n/a
2212C10	0.997	0.986	CPM	1.671	1.036	89.530	yes	yes
2212C11	0.999	0.999	CPM	1.714	1.274	89.917	yes	yes
2212C12	1.000	1.000	CPM	0.766	0.827	89.992	yes	n/a
2212C13	0.987	0.996	CPM	1.713	1.601	88.974	yes	yes
2212C14	0.998	0.996	CPM	0.726	14.471	89.750	yes	no
2212C15	0.999	1.000	CPM	0.828	0.863	89.925	yes	no

2212C16	0.985	0.995	CPM	1.182	1.698	88.825	yes	n/a
2212C17	0.986	0.996	CPM	0.773	3.126	88.892	yes	n/a
2212C18	0.999	0.974	CPM	1.337	24.883	89.521	yes	no
2212C19	0.994	0.997	CPM	0.630	1.408	89.473	yes	n/a
2212C20	1.000	0.998	CPM	1.399	n/a	89.943	yes	n/a

5. Conclusions

Several possible physical pairs are hidden in the night sky. Amateur astronomers with the appropriate skills and knowledge in data analysis, astronomical imaging and a lot of enthusiasm have the opportunity to access really useful data in different sky surveyor programs like Gaia, to identify new possible candidates. However, the accuracy of the actual data available in Gaia DR3 database is limited, therefore it is not possible to determine the nature of several double stars. Future data releases will support this work to a greater extent.

Acknowledgements

Special thanks to Tamas Ladanyi, the leader of the Hungarian Astronomical Association Double Star Section (email: tom.ladanyi@gmail.com) and to Zsolt Szamosvari, member of the Hungarian Astronomical Association Double Star Section.

This research has made use of the Washington Double Star Catalog maintained at the U.S. Naval Observatory.

This work has made use of data from the European Space Agency (ESA) mission Gaia (https://www.cosmos.esa.int/gaia), processed by the Gaia Data Processing and Analysis Consortium (DPAC, https://www.cosmos.esa.int/web/gaia/dpac/consortium). Funding for the DPAC has been provided by national institutions, in particular the institutions participating in the Gaia Multilateral Agreement.

This work has made use of The Astropy Project: Sustaining and Growing a Community-oriented Open-source Project and the Latest Major Release (v5.0) of the Core Package (Astropy Collaboration et al. 2022.); the The Astropy Project: Building an inclusive, open-science project and status of the v2.0 core package (Astropy Collaboration et al. 2018.) and the Astropy: A community Python package for astronomy (Astropy Collaboration et al. 2013.)

This research made use of Photutils, an Astropy package for detection and photometry of astronomical sources (Bradley et al. 2022.).

This research has made use of "Aladin sky atlas" developed at CDS, Strasbourg Observatory, France → 2000A&AS..143...33B and 2014ASPC..485..277B.

This research has made use of " SkyChart / Cartes du Ciel " developed by Patrick Chevalley. Retrieved from https://www.ap-i.net/skychart/en/start.

References

Harris, C.R., Millman, K.J., van der Walt, S.J. et al. Array programming with NumPy. Nature 585, 357–362 (2020). DOI: 10.1038/s41586-020-2649-2. (Publisher link).

Espin, T. E., & Milburn, W. (1927). Micrometrical Measures of Double Stars (21st Series). Monthly Notices of the Royal Astronomical Society, 87(3), 215–225. https://doi.org/10.1093/mnras/87.3.215.

Knapp, W. R., & Nanson, J. (2018). Estimating Visual Magnitudes for Wide Double Stars with Missing or Suspect WDS Values. Journal of Double Star Observations, Vol. 14 No. 3. Page 503. Retrieved from http://www.jdso.org/volume14/number3/Knapp_503_520.pdf

Harshaw, R. (2016). CCD Measurements of 141 Proper Motion Stars: The Autumn 2015 Observing Program at the Brilliant Sky Observatory, Part 3. Journal of Double Star Observations, Vol. 12 No. 4. Page 394. Retrieved from http://www.jdso.org/volume12/number4/Harshaw_394_399.pdf

[1], [2] Harshaw, R. (2018). Gaia DR2 and the Washington Double Star Catalog: A tale of two databases. Journal of Double Star Observations, Vol. 14 No. 4. Page 734. Retrieved from http://www.jdso.org/volume14/number4/Harshaw_734_740.pdf

M. I. Nouh & M. A. Sharaf (2012). On the Maximum Separation of Visual Binaries. Journal of Astrophysics and Astronomy, Volume 33, Issue 4, pp.375-386. Retrieved from https://www.researchgate.net/publication/257766465_On_the_Maximum_Separation_of_Visual_Binaries

[6] F.M. Rica (2011). Determining the Nature of a Double Star: The Law of Conservation on Energy and the Orbital Velocity. Journal of Double Star Observations, Volume 7. No 4. Page 254. Retrieved from http://www.jdso.org/volume7/number4/Rica_254_259.pdf

L. Dugan et al. (2022). STF 42 AB Measuring and Reclassification. Journal of Double Star Observations, Volume 18. No 4. Page 14. Retrieved from http://www.jdso.org/volume18/number4/Dugan_357_363.pdf

K. Sturrock (2021). Description of a CCD Astrometric Double Star Survey System, The Webb Deep-Sky Society Double Star Section Circular No. 29., Page 19. Retrieved from https://www.webbdeepsky.com/dssc/dssc29.pdf.